

## Supplementary Materials for

### Structural photoactivation of a full-length bacterial phytochrome

Alexander Björling, Oskar Berntsson, Heli Lehtivuori, Heikki Takala, Ashley J. Hughes, Matthijs Panman, Maria Hoernke, Stephan Niebling, Léocadie Henry, Robert Henning, Irina Kosheleva, Vladimir Chukharev, Nikolai V. Tkachenko, Andreas Menzel, Gemma Newby, Dmitry Khakhulin, Michael Wulff, Janne A. Ihalainen, Sebastian Westenhoff

Published 12 August 2016, *Sci. Adv.* **2**, e1600920 (2016)  
DOI: 10.1126/sciadv.1600920

#### This PDF file includes:

- table S1. SAXS parameters.
- table S2. Ab initio modeling.
- fig. S1. Time-resolved absorption spectra.
- fig. S2. Decay-associated spectra extracted from time-resolved absorption spectroscopy.
- fig. S3. Concentration dependence of x-ray scattering data and Guinier fits.
- fig. S4. SAXS data in Pr and Pfr.
- fig. S5. Comparison of reconstructed envelopes and the structural model from the study of Dago *et al.* (52).

**Table S1.** SAXS parameters. Parameters pertaining to the Pr state were derived from a absolute scattering dataset at 1 mg/ml protein concentration (34). The Pfr parameters were derived from reconstructed absolute scattering curves, which were recorded at a protein concentration of 7.2 mg/ml. The parameters  $R_g$  and  $I_0$  were estimated using conventional Guinier analysis as well as from the pair distance distribution function. The values corresponding to the experimentally determined  $\alpha = 0.38$  are marked in bold. Even for a low value of  $\alpha = 0.13$ , the change of  $R_g$  was still small with  $\Delta R_g < 0.5 \text{ \AA}$ . The change in  $V_c$  was moderate with  $\Delta V_c < 3\%$  and mainly caused by a change in  $I_0$ .

Parameter	Pr	Pfr( $\alpha=0.45$ )	<b>Pfr(<math>\alpha=0.38</math>)</b>	Pfr( $\alpha=0.32$ )	Pfr( $\alpha=0.26$ )	Pfr( $\alpha=0.19$ )	Pfr( $\alpha=0.13$ )
Rg (Guinier) ( $\text{\AA}$ )	53.25 ( $\pm 0.05$ )	53.32 ( $\pm 0.05$ )	<b>53.27 (<math>\pm 0.05</math>)</b>	53.19 ( $\pm 0.1$ )	53.23 ( $\pm 0.1$ )	53.01 ( $\pm 0.1$ )	52.69 ( $\pm 0.1$ )
I( $q=0$ ) (Guinier)	37.6	36.7	<b>36.5</b>	36.3	36	35.4	34.2
Rg (P(r)) ( $\text{\AA}$ )	53.96 ( $\pm 0.05$ )	53.89 ( $\pm 0.05$ )	<b>53.87 (<math>\pm 0.05</math>)</b>	53.85 ( $\pm 0.06$ )	53.72 ( $\pm 0.06$ )	53.66 ( $\pm 0.05$ )	53.6 ( $\pm 0.05$ )
I( $q=0$ ) (P(r))	37.6	36.7	<b>36.5</b>	36.3	36.0	35.4	34.3
$V_{\text{Porod}}$ ( $\text{nm}^3$ )	353	351	<b>350</b>	350	350	348	346
$V_c$ ( $\text{\AA}^2$ )	1139	1131	<b>1129</b>	1127	1125	1118	1107
MW ( $Q_R$ ) (kDa)	195	193	<b>192</b>	191	191	189	186
MW (BSA) (kDa)	168	164	<b>163</b>	162	161	158	153
MW (calc.) (kDa)	168	168	<b>168</b>	168	168	168	168
$D_{\text{max}}$ ( $\text{\AA}$ )	186	186	<b>186</b>	186	186	186	184

**Table S2.** Ab initio modelling. In the first modelling round 20 models were generated and compared. The result was then used to generate 10 new models in round 2. The models with smallest mean NSD respectively was compared to the final Pr state model.

Dataset	Round 1		Round 2		Final	
	Rejected	Mean NSD (stdev.)	Rejected	Mean NSD (stdev.)	$\chi$	NSD vs Pr
Pr	2	0.616 (0.038)	0	0.198 (0.003)	1.113	0.000
Pfr( $\alpha=0.45$ )	0	0.659 (0.025)	0	0.215 (0.013)	1.308	0.857
Pfr( $\alpha=0.38$ )	1	0.666 (0.045)	0	0.476 (0.029)	1.373	0.785
Pfr( $\alpha=0.32$ )	0	0.679 (0.045)	1	0.505 (0.029)	1.482	0.841
Pfr( $\alpha=0.26$ )	1	0.677 (0.049)	1	0.224 (0.011)	1.525	0.739
Pfr( $\alpha=0.19$ )	0	0.683 (0.042)	0	0.485 (0.032)	1.856	0.957
Pfr( $\alpha=0.13$ )	1	0.677 (0.038)	1	0.167 (0.007)	2.719	0.960

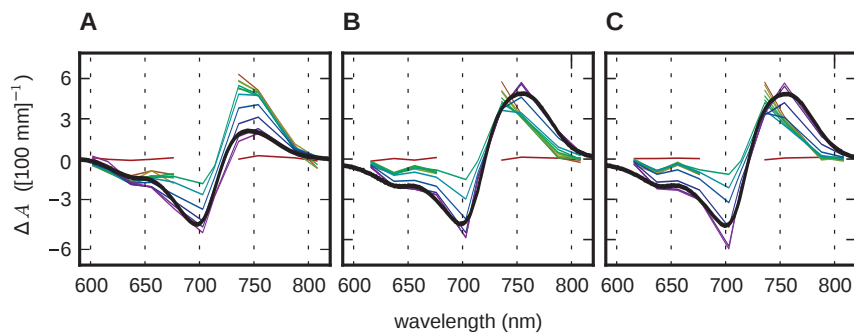


**fig. S1.** Time-resolved absorption spectra. Colors represent the same delays as in Fig. 3. Experimental details are described in Materials and Methods.

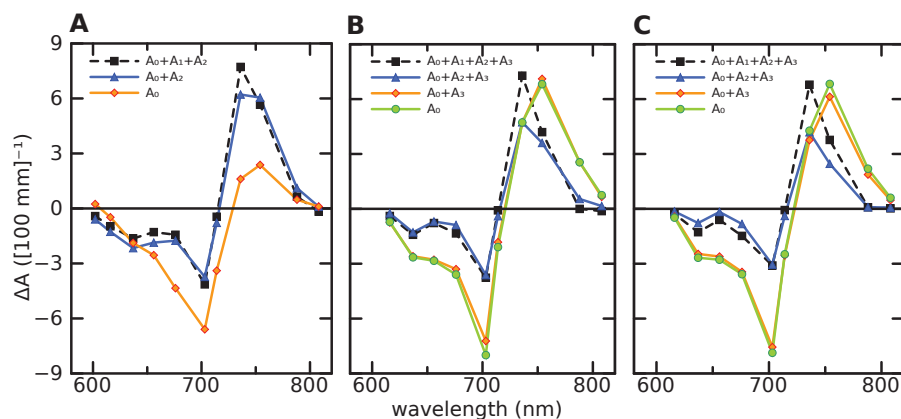


**fig. S2.** Decay-associated spectra extracted from time-resolved absorption spectroscopy, as described in Materials and Methods. Overall the decay-associated spectra of *D. radiodurans* indicate a photocycle similar to that of the *A. tumefaciens* phytochrome (25, 26), but the details are different. All samples have a similar spectral evolution with the 53 (55, 80)  $\mu\text{s}$  time constant. This is in line with the changes being internal to the chromophore binding domains. The component is assigned to the formation of the meta-Ra state. The next component ( $A_2$ ) has a similar spectral shape in the PAS-GAF-PHY and FL proteins, but the shape for PAS-GAF is different. This is in agreement with the idea that the PHY-arm is involved in this transition. In the *A. tumefaciens* and *Synechocystis sp.* phytochromes, proton release was observed for this transition (24, 25) and the component was assigned to the meta-Ra to meta-Rc transition. The last time constant in PAS-GAF-PHY is 200 ms ( $A_3$ ), but its associated spectrum is very small in amplitude. The spectral component has no resemblance in the *A. tumefaciens* data and remains unassigned (26). The spectral shape of the last component for FL ( $A_3$ ), with a lifetime of 27 ms, is similar to the last in-growth of far-red absorption in *A. tumefaciens* (25) and is a signature of the meta-Rc to Pfr transition.

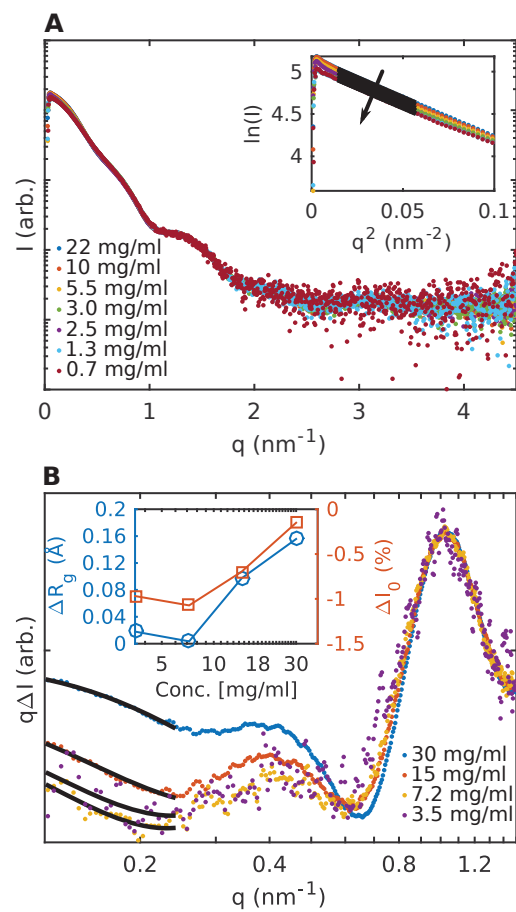


**fig. S3.** SAXS data collected at different concentrations (A) and the corresponding Guinier ranges and linear fits as black lines (A, inset), concentration is decreasing along the arrow. Difference scattering data collected at different concentrations with the fitted Guinier ranges in black (B) and the concentration dependence of  $R_g$  and  $I_0$  (B, inset).  $I_0$  is given in % relative to the  $I_0$  for Pr.

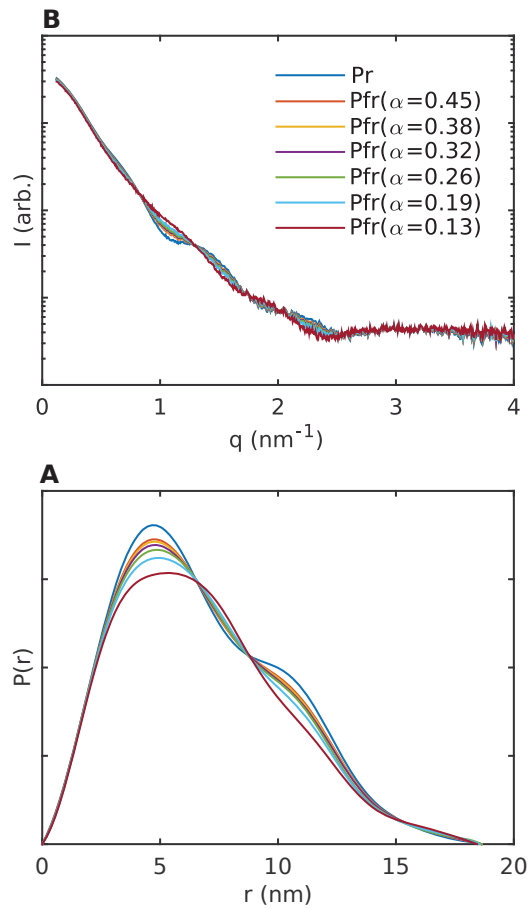


**fig. S4.** SAXS data measured for Pr and reconstructed for Pfr assuming different values of  $\alpha$  (A) and the corresponding pair distance distribution functions (B).

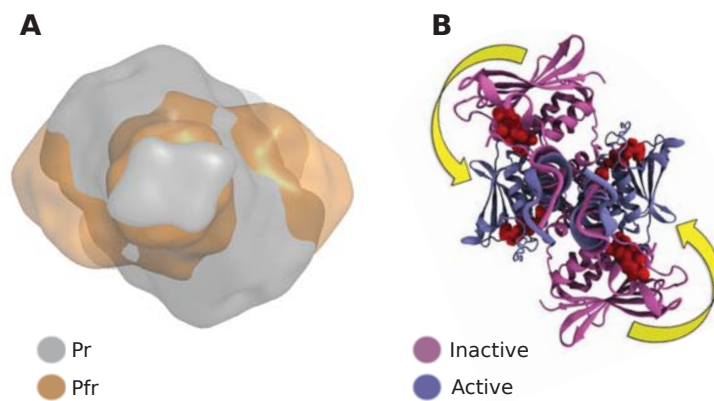


**fig. S5.** Top view of SAXS derived envelopes (A) and the structural change for histidine kinases suggested by Dago et al., adapted from (49) (B).